Synthesis of dense nanometric MoSi2 through mechanical and field activation

Orru, R.V.A.; Woolman, J.; Cao, G.; Munir, Z.A.

document version
Publisher's PDF, also known as Version of record

Synthesis of dense nanometric MoSi$_2$ through mechanical and field activation

R. Orrù
Facility for Advanced Combustion Synthesis, Department of Chemical Engineering and
Materials Science, University of California, Davis, California 95616, and
Dipartimento di Ingegneria Chimica e Materiali, Università di Cagliari, Piazza d'Armi, 09123,
Cagliari, Italy

J. Woolman
Facility for Advanced Combustion Synthesis, Department of Chemical Engineering and
Materials Science, University of California, Davis, California 95616

G. Cao
Dipartimento di Ingegneria Chimica e Materiali, Università di Cagliari, Piazza d'Armi, 09123,
Cagliari, Italy

Z.A. Munir[a]
Facility for Advanced Combustion Synthesis, Department of Chemical Engineering and
Materials Science, University of California, Davis, California 95616

The effect of mechanical and field activation on the synthesis of dense nanometric MoSi$_2$ was investigated. Powders of Mo and Si, milled separately or comilled in a planetary ball mill, were reacted in a spark plasma synthesis (SPS) apparatus under different electric current conditions. Milled powders reacted faster and required less current than unmilled powders. Mixtures of powders which were milled separately (to nanometric size) reacted in the SPS to produce micrometric α–MoSi$_2$. Similar results were obtained for samples comilled to produce nanometric reactants which did not contain detectable amounts of the product phase. When products form during milling, they contain both the α and β modifications of MoSi$_2$. The product after the SPS reaction was nanometric MoSi$_2$ with a crystallite size of 140 nm.

I. INTRODUCTION

The synthesis of molybdenum disilicide has been accomplished by a variety of methods, including arc melting, combustion synthesis (SHS), and mechanical alloying. The product of mechanical alloying is typically an agglomerated powder while that of the SHS process is usually a porous solid. In a more recent study, Gras *et al.*[1] combined these two approaches by milling powders of Mo and Si an then reacting them by the SHS method. They reported the product to be nanometric α–MoSi$_2$. However, the synthesized silicide was highly porous, as is the case in the majority of materials prepared by this method. Obviously in many cases the practical advantages of nanomaterials can only be realized when highly dense products can be made. The process of making dense nanomaterials, however, is not simple, as will be discussed subsequently. It has been suggested that the scarcity of adequate mechanical properties on

nanomaterials is the consequence of the difficulty of preparing high-density samples.[2] The feasibility of a new approach for the simultaneous synthesis and densification of nanomaterials has been recently demonstrated.[3–5] In this paper we report the results of an investigation on the synthesis of dense nanometric MoSi$_2$

By far the majority of investigations on the synthesis of this silicide were those focused on the effect of milling on the formation of a nanometric product. In these investigations, two types of mills were employed: SPEX and planetary mills. Using the former type, Schwarz *et al.*[6] reported the formation of MoSi$_2$ after 20 h of milling under an unspecified condition of charge ratio (CR), i.e., ball/power mass ratio. But even after this time, unreacted Mo was still observed. From x-ray analyses on the product, they calculated a crystallite size for MoSi$_2$ of 10–15 nm. Subsequent hot-pressing of this material resulted in 97% dense bodies, but the densification process was accompanied by a very large grain growth. The grain size increased by more than 3 orders of magnitude after 20–30 min at 1500 °C. Using a similar experimental approach, Ma *et al.*[7] reported the near complete formation

[a]Address all correspondence to this author.

of the low temperature (α) form of the silicide after 3 h of milling with CR = 5. The product, however, had a large particle size, in the range of one to few hundred micrometers. These authors reported that the formation of α–MoSi$_2$ is abrupt and concluded that the process is a self-sustaining combustion. Similar conclusions were made by Patankar *et al.*[8] on the basis of the abrupt dependence of the formation of the silicide phase on time. Product formation (under CR = 10) occurred within a time increment of about 1 min after milling for 3.22 h (193 min). The crystallite size of the product was reported to be 300 nm. But in a more recent investigation using the same technique, the formation of MoSi$_2$ was not detected until after 20 h of milling. Even then, unreacted Mo was still present and persisted after 40 h of milling time.[9]

The published results of the planetary milling investigations are also varied with regards to the formation of the product. Fei *et al.*,[10] using a relatively high CR of 15, reported that the complete formation of the silicide is not achieved until after 210 h of milling. Continued milling for 300 h resulted in a product with a crystallite size of 43 nm. The need for longer times to form MoSi$_2$ in a planetary mill was also confirmed in another study in which no product formed after 40 h of milling with CR = 5.[11] In contrast, Bokhonov *et al.* reported the formation of α–MoSi$_2$ after 6 min of milling.[12] In their work, however, the charge ratio was significantly higher (CR = 20) than in the other cases.

In all of the above examples the products are either agglomerated powders or, in the case of the SHS study,[1] porous bodies. Except for the case of thin film formation by CVD or PVD, the preparation of dense nanomaterial requires an additional step. Consolidation of nanopowders to product dense bodies for further property characterization has been accomplished with several techniques including sintering, hot-pressing, and spark plasma (or pulsed electric current) sintering (SPS).[13–18] The major concern in all of these methods of consolidation is grain growth. In view of the nonequilibrium state of the nanomaterials and the fact that consolidation takes place at high temperatures and requires relatively long holding times, grain growth (Oswald ripening) is anticipated. In the cited study of Schwarz *et al.*,[6] the grain size increased from a range of 10–15 nm to 3–10 μm during the 20–30 min of densification by hot-pressing with 12 MPa at 1500 °C. As was pointed out above, the relatively limited number of experimental data on mechanical and plastic properties on nanomaterials has been attributed to the difficulty of synthesizing dense bodies.[2]

Thus the preparation of dense nanomaterials has until recently been a two-step process involving the sequential synthesis and consolidation. A few years ago, a process was developed to simultaneously synthesize and densify materials using electric field activation.[19,20]

More recently, this approach was extended to the synthesis of dense nanomaterials.[3–5] In the present investigation the simultaneous synthesis and densification of MoSi$_2$ using mechanically activated elemental reactants was studied.

II. EXPERIMENTAL MATERIALS AND METHODS

A. Ball milling and x-ray diffraction analysis

The starting powders used in the present investigation were commercially available Mo (Alfa Aesar, 3–7 μm, 99.95% purity) and Si (Alfa Aesar, −325 mesh, 99.5% purity). Elemental powders were milled either separately or together (comilled) in a stoichiometric ratio corresponding to MoSi$_2$. Ball-milling experiments were conducted in a planetary ball mill (Fritsch model Pulverisette 5) using zirconia vials and 50 zirconia balls (10 mm in diameter). In order to minimize oxidation, all powder handling and loading were performed inside a glovebox which had been evacuated and back-filled with argon gas. The vials were then sealed and transferred to the ball mill. Milling runs included repeated cycles of 1 h of milling followed by 1 h of cooling. After each run, the powders were removed and the vials and balls were cleaned using a slurry of silica and methanol in order to remove all residual powders of the previous milling experiment. The range of the charge ratio, CR (ball to powder mass ratio), investigated was 7–21. A ball milling rotation speed, *R,* of 250 rpm was generally used but the effect of a further increase of the rotation speed (300 rpm) was also investigated.

Phase identification and crystallite size evolution during the milling process were obtained using a Scintag XDS 2000 x-ray diffractometer with Cu K$_\alpha$ radiation (λ = 1.5405 Å). No Ni filter was used in order to minimize the reduction in peak intensity. Minor peaks were also detected from Cu K$_\beta$ (λ = 1.3922 Å) and W L$_\alpha$ (λ = 1.4763 Å) radiation. Crystallite size was determined using the Williamson–Hall method[21] from the line broadening of x-ray diffraction peaks. This method makes it possible to separate the two contributions to line broadening, namely, the refinement of crystallite size and the internal strain. The full width at half-maximum, $B(h)$, was obtained by fitting the highest intensity diffraction peaks after correcting for the K$_{\alpha_2}$ contribution to the peak width. The choice of the function to be used for the fitting of the measured diffraction peaks was done on the basis of preliminary test results obtained using Lorentzian, Gaussian, Voigt, and Pearson curves.[22] This investigation demonstrated that the Pearson fit gave the best fit for the present result.

To isolate only the contribution of the examined sample, i.e., the half-maximum breadth of the true diffraction profile, $B(f)$, the measured breadth, $B(h)$, were

corrected for instrumental contribution, $B(g)$, i.e., $B(f) = B(h) - B(g)$. The value of $B(g)$ was determined from the diffraction profile of a strain-free, well-annealed, coarse-grained specimen of LaB$_6$. As suggested in the literature,[22] the variation of $B(g)$ versus θ was obtained by fitting the measured breadth of the diffraction peaks of the standard material, using the following polynomial function:

$$[B(g)]^2 = U \tan^2 \theta + V \tan \theta + W \quad , \quad (1)$$

where U, V, and W are constants.

As mentioned above, we employed the method of Williamson and Hall, where the broadening contribution of the diffraction lines due to strain and to crystallite size are combined as follows:

$$B(f) = \eta \tan \theta + \frac{k\lambda}{L \cos \theta} \quad , \quad (2)$$

where L is the crystallite size, η is the strain, θ is the Bragg angle, k is the Scherrer constant which has been set equal to one, and λ is the x-ray wavelength. Thus, by the plotting of $B(f) \cos(\theta)$ versus $\sin(\theta)$ [or alternatively, as typically found, the plotting of $B*(f) = B(f) \cos(\theta)/\lambda$ as a function of $d* = 2 \sin(\theta)/\lambda$], a straight line is obtained. The intercept of this line gives the inverse of the average crystallite size, L, and its slope provides the value of the strain.

B. Field-activated synthesis and consolidation of milled powders

The experimental facility employed to simultaneously react and consolidate the milled powders was the spark plasma sintering (SPS) system (model SPS-1050, Sumitomo Mining Company, Ltd., Kawasaki, Japan). This apparatus combines a 100 kN uniaxial press with a 15 V, 5000 A dc power supply to provide a pulsed current through the sample and the die that contains it. The pulse cycle is 12 ms on and 2 ms off. Other than providing rapid Joule heating, the imposed pulsed high current is reported to generate a plasma within the voids surrounding the powder particles.[23] It is also likely that the presence of the current enhances mass transport through electromigration.[24]

The reactants were stoichiometric mixtures of Mo and Si powders which were either comilled or milled separately and then blended by Turbula mixer for 6 h. For a comparison, as-received (unmilled) reactant powders were also used. In this case, the treatment of the commercial Mo and Si powders constituted only the mixing in the Turbula for 6 h. In each case, 7 g of powder mixture was placed in a graphite die (internal diameter = 19 mm) which was lined with graphite foil. However, no foil was used between the sample and the graphite plungers. The die was then placed inside the

reaction chamber of the SPS apparatus, and the system was evacuated. This step was followed by the application of an 18-kN load through the plungers, which corresponds to a pressure of 63.5 MPa.

The experiment is initiated with the application of a previously set constant value of the electric power setting which is directly proportional to the maximum current of 5000 A. The electric power range investigated is 17–25% $P_{\max}$ (nominally a current range of 850–1250 A). The temperature of the external surface of the graphite die was measured by a pyrometer. Voltage, current, load, sample displacement, and displacement rate were measured in real time during synthesis. Although some consolidation takes place immediately after the application of the load, the most significant and typically rapid volume change accompanies the onset of the reaction. Therefore sample displacement constitutes an important indication of the onset of the reaction between Mo and Si. Typically, the power was turned off as soon as the rapid displacement occurred.

After the reaction, the sample was allowed to cool before it was removed from the die. The relative density of the product was determined by geometrical measurements and by the Archimedes method. Phase identification and crystallite size analysis of the consolidated samples were made using XRD analyses.

III. RESULTS AND DISCUSSION

A. Ball milling and x-ray analysis

1. Elemental powders milled separately

Figure 1(a) shows the variation of the XRD patterns for Mo powder with milling time for the conditions of $R = 250$ rpm and CR = 7. It should be noted that the two small peaks with 2θ in the range 36.4–38.8° in this and subsequent XRD figures are due to instrumental contributions from Cu K$_\beta$ and W L$_\alpha$ diffractions, as indicated in the Experimental section. With increasing milling time the initially sharp diffraction peaks become broader and their intensity decreases. Figure 1(b) shows the x-ray patterns of Si powders milled for different times at the same conditions. Again, the two small peaks in the 2θ range of 25–28° in this and subsequent figures are from the instrumental contributions of the Cu K$_\beta$ and W L$_\alpha$ for Si, as indicated before. In contrast to the case of Mo, as milling time increases, only small changes are observed in the intensity and width of the diffraction peaks. However, an increase in CR has a much more pronounced effect on the intensity of the peaks of Si than those of Mo, as seen in Figs. 2(a) and 2(b). In both cases, the conditions are $R = 250$ rpm, and $t = 8$ h. In addition, it is worth noting that the background line of XRD pattern corresponding to the milled Si also becomes more

intense when increasing the charge ratio, Fig. 2(b). The effect of changing the rotational speed on the XRD patterns for Mo and Si is shown in Figs. 3(a) and 3(b), respectively. The patterns are of powders milled under two different rotational speeds of $R = 250$ and 300 rpm with all other conditions being identical. The diffraction peak intensities of Mo decrease slightly and the peak widths increase slightly as the speed is increased. But for the case of Si only a small variation in the XRD patterns of the milled powders with R is seen. The dependence of the calculated crystallite size of Mo, $L,$ on milling time for three CR ratios is shown in Fig. 4.

2. Elemental powders milled together

The variation of the x-ray diffraction patterns of the stoichiometric powder mixtures (1 Mo:2 Si) with milling time for CR = 7 and $R = 250$ rpm is shown in Fig. 5. This result indicates, within the detection limit of this analysis, that a product is not formed at milling times less than 9 h. Furthermore, an increase in milling time was found to have a stronger effect on the Si peaks than on the Mo peaks. With increasing milling time, the Si peaks broaden and their intensity decreases rapidly. Si reflections almost disappeared at a point corresponding to the first evidence of formation of the product phase, MoSi$_2$. In contrast, while the observed Mo diffraction peaks became broader and less intense with milling time, this
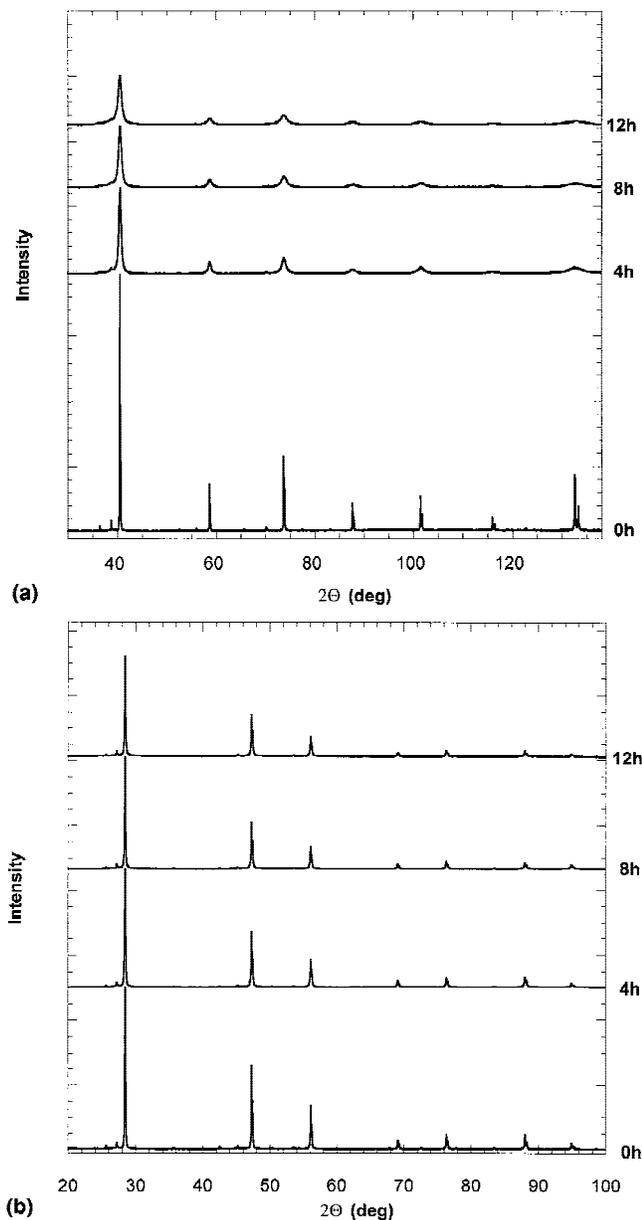

FIG. 1. (a) XRD patterns of Mo as a function of milling time ($R = 250$ rpm, CR = 7). (b) XRD patterns of Si as a function of milling time ($R = 250$ rpm, CR = 7).
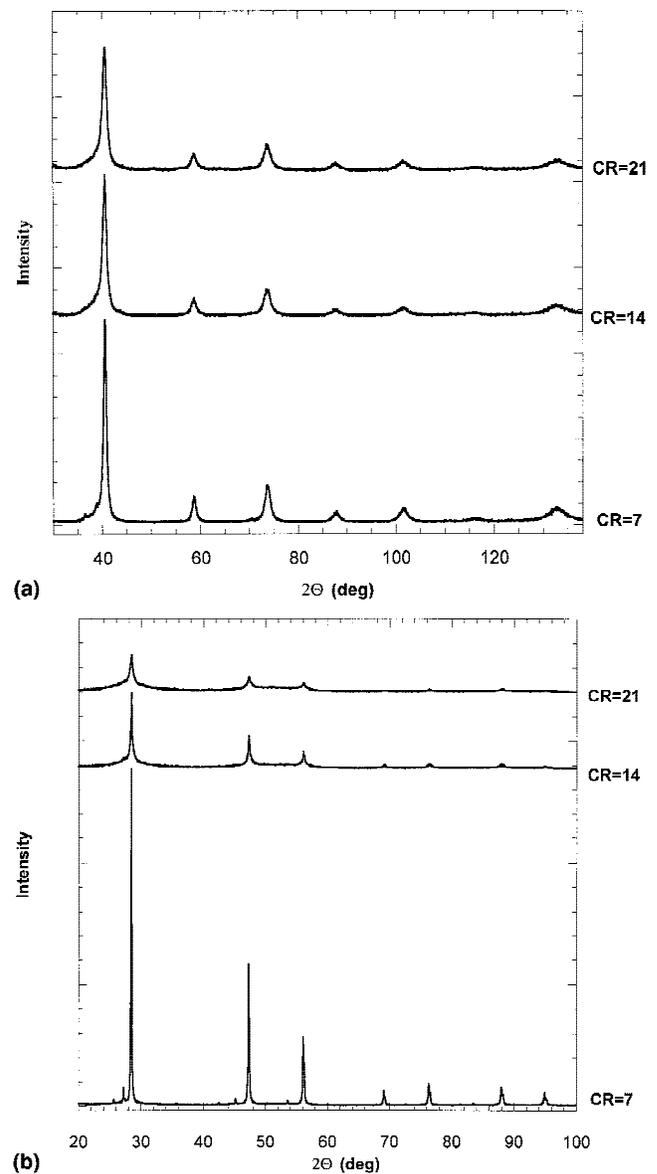
FIG. 2. (a) XRD patterns of Mo as a function of charge ratio ($R = 250$ rpm, $t = 8$ h). (b) XRD patterns of Si as a function of charge ratio ($R = 250$ rpm, $t = 8$ h).

effect is relatively insignificant compared to that for the Si. The reduction in the intensity of the Si peaks with milling is in agreement with previous observations.[6,7] It was suggested that the reduction is the consequence of the dissolution of Si in Mo or the formation of the silicide phase. The fact that in our study no such observation was made on Si powders milled separately would lend support for the proposed explanation. The disappearance of the Si peaks coincided with the appearance of the peaks of the product phase.

Figure 6 depicts XRD patterns of powders milled at varying CR values for $R = 250$ rpm and a milling time of 3 h. Under these conditions, disilicides reflections
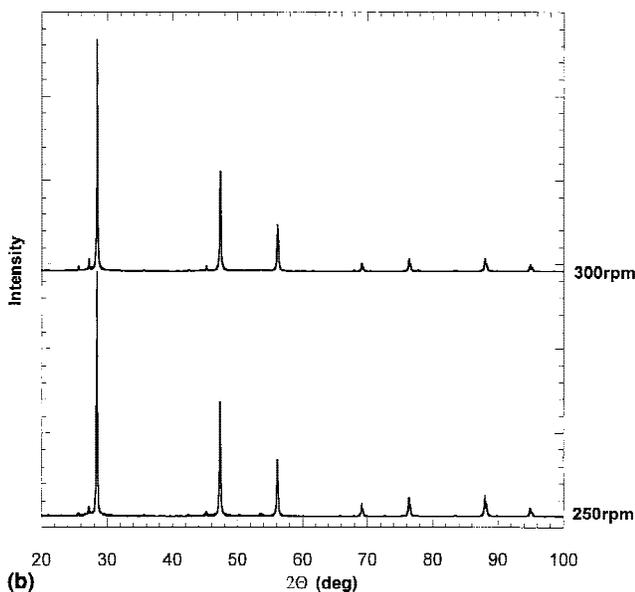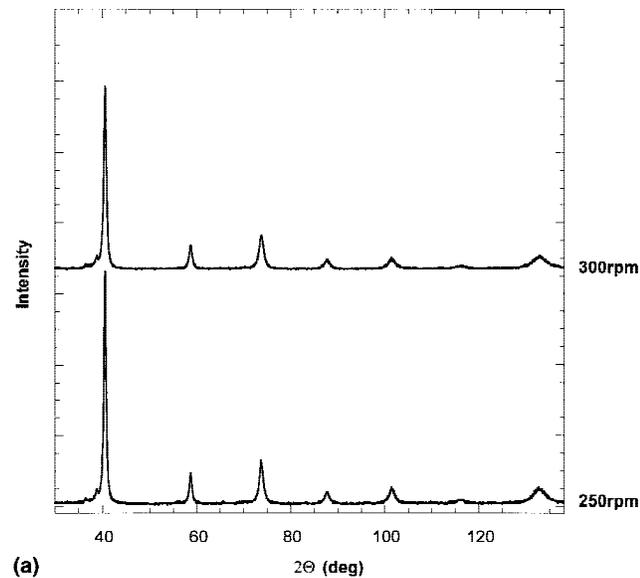
began to appear (after 3 h) when CR = 16. Analogous results were obtained at different milling times. Figure 7 summarizes the results of the conditions under which product phase formation occurs for $R = 250$ rpm. The milling time required for product formation decreases as CR increases. The dashed line in the figure represents the boundary separating the region of product formation from the region where only the reactants are detected by XRD analysis. There is experimental evidence (see
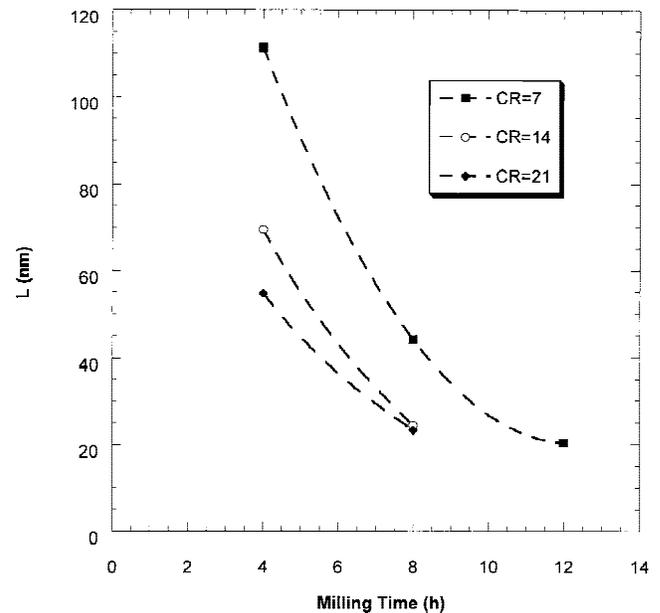

(a)

FIG. 4. Dependence of Mo crystallite size on milling time at different charge ratios ($R = 250$ rpm).

(b)

FIG. 3. (a) XRD patterns of Mo as a function of rotational speed ($t = 4$ h, CR = 7). (b) XRD patterns of Si as a function of rotational speed ($t = 4$ h, CR = 7).
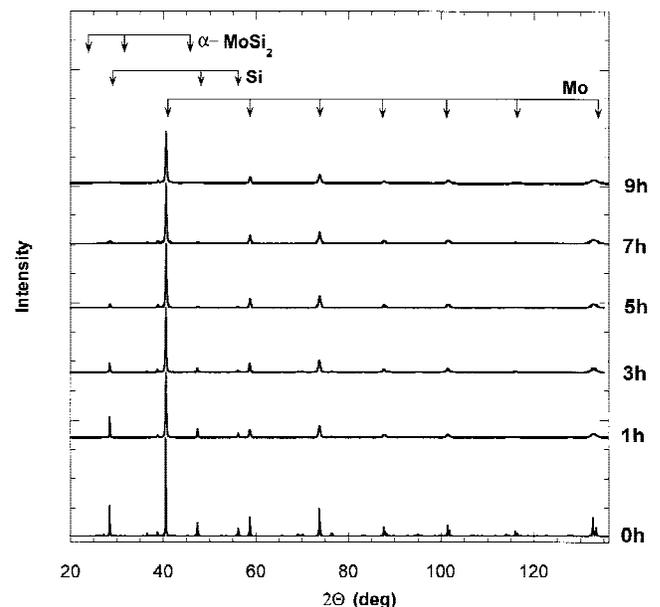

FIG. 5. XRD patterns of blended Mo + 2 Si powders as a function of milling time ($R = 250$ rpm, CR = 7).

below) that such a boundary is dependent on the rotational speed, *R*. But with reference to the data of Fig. 7, it was found, using the Williamson–Hall analysis, that the smallest molybdenum crystallite size obtained before product formation commenced, is when $t = 3$ h and CR = 14 (for $R = 250$ rpm). The corresponding crystallite size was 125 nm. However, since under these milling conditions the silicon peaks almost disappeared from the XRD pattern, no crystallite size analysis could be made for Si.
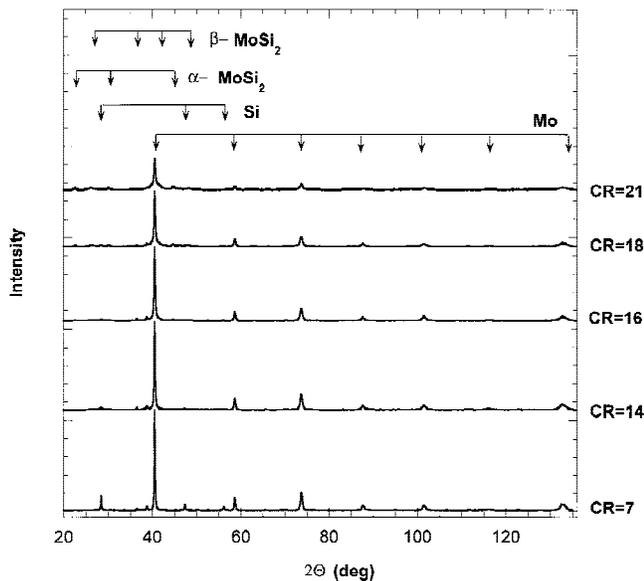

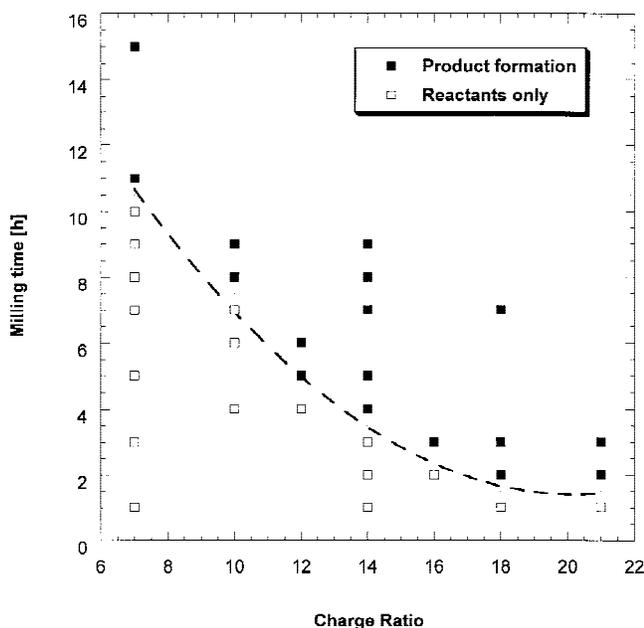FIG. 6. XRD patterns of milled Mo + 2 Si powders as a function of charge ratio ($R = 250$ rpm, $t = 3$ h).

The effect of changing the rotational speed, *R,* from 250 to 300 rpm for a case of CR = 7 and $t = 7$ h is shown in Fig. 8. As *R* increases, Si peak intensity decreases with an almost insignificant change in the Mo peaks. Moreover, there is an indication of the beginning of formation of α–MoSi₂. As indicated above, this implies that the boundary delineating product formation (see Fig. 7) is a function of the parameter *R*.

B. Synthesis reaction and consolidation of milled powders

It was found that milling of the reactants has a direct influence on the subsequent reactivity in the SPS. For example, when unmilled powder mixtures of Mo + 2 Si were subjected to a 20% P_{max} (925 A), no reaction occurred even after the imposition of this current for 20 min. Details of the effect of milling as well as the parameters of the SPS process on the reactivity of these powders are described in another paper.[25] When comilled powders were used (at $R = 250$ rpm, $t = 3$ h, and CR = 14), a reaction in the SPS does take place at this low power value (17% P_{max}). Figures 9(a)–9(c) show the SPS and XRD results. The current increases in about 4 s to a value of 750 A [Fig. 9(a)], somewhat less than the expected maximum for this power setting, but that is related to the other events taking place. However, an abrupt displacement (totaling 3 mm) takes place after only 1.5–2.5 s from the application of the electric power [Fig. 9(b)]. This event happened when the current was in the range 400–600 A. No temperature was recorded by the pyrometer, indicating that the temperature at the
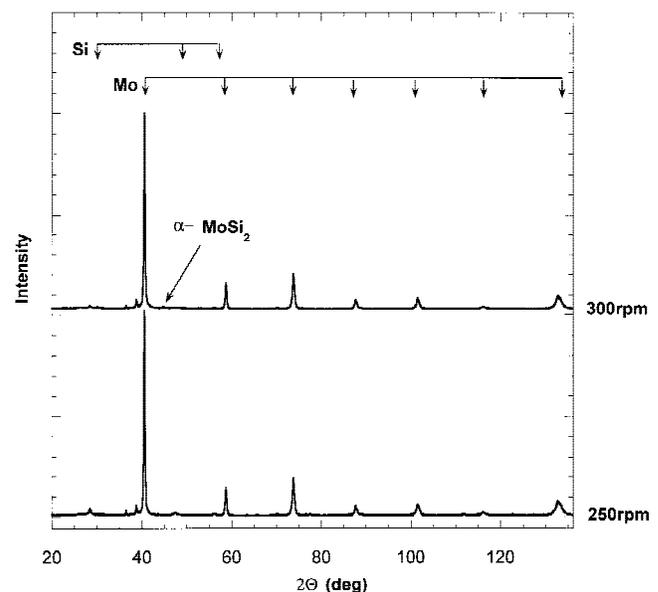

FIG. 7. Effect of milling time and charge ratio on product formation ($R = 250$ rpm).

FIG. 8. XRD patterns of milled Mo + 2 Si powders as a function of rotational speed ($t = 7$ h, CR = 7).
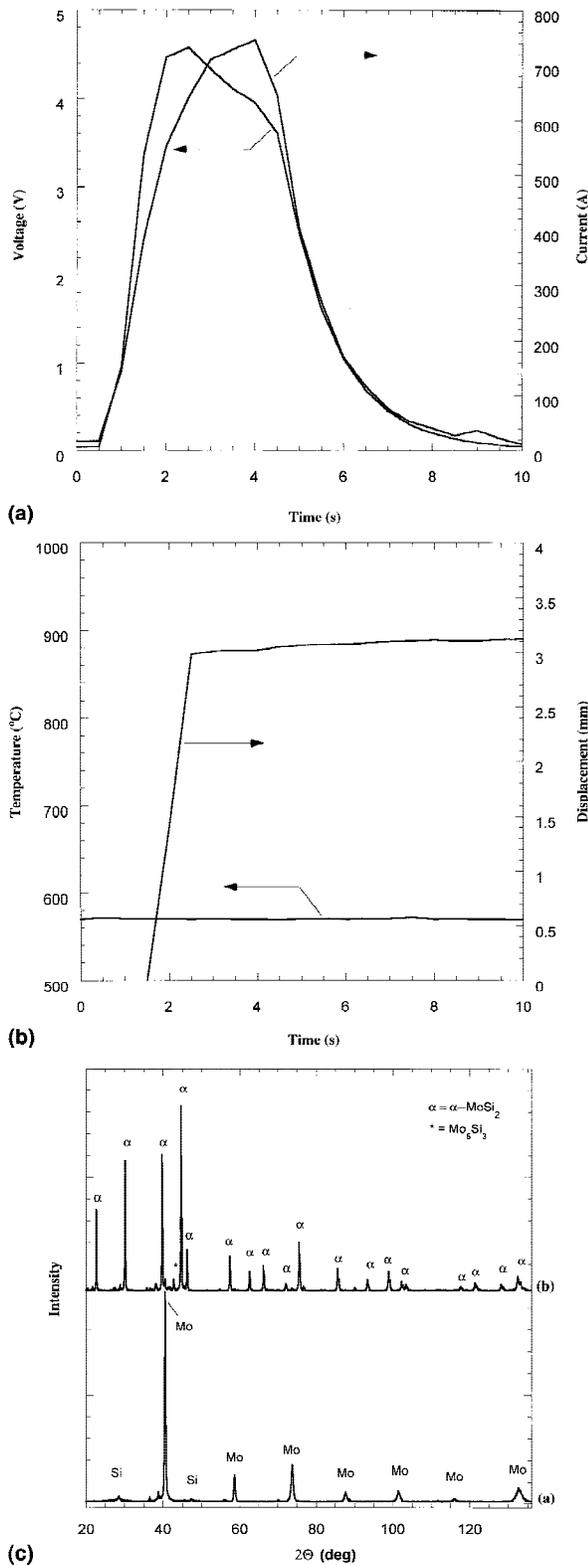
FIG. 9. (a) Voltage and current changes during SPS experiments for Mo + 2 Si milled powders (R = 250 rpm; t = 3 h; CR = 14); P = 17% P_{max}. (b) Temperature and sample displacement changes during SPS experiments for Mo + 2 Si milled powders (R = 250 rpm; t = 3 h; CR = 14); P = 17% P_{max}. (c) XRD patterns of SPS reacted powders milled under the same conditions as in (a).

surface of the die is less than the lower limit of this instrument, 650 °C. A comparison between the XRD patterns of the starting milled powder mixture and the final product is shown in Fig. 9(c). The reactants have almost completely converted to α-MoSi$_2$. Some traces of Mo$_5$Si$_3$ are also found, but there is no evidence for the presence of β–MoSi$_2$. However, the diffraction peaks of the product appear to be narrow indicating a relatively large crystallite size. This was confirmed by crystal size analysis which revealed that the grain size was about 1–2-μm size. Thus when nanometric reactants which did not contain any measurable amounts of the product phase were reacted in the SPS, the product was not nanometric. This is in agreement with published results in which it was found that the presence of small (unspecified) amounts of the product phase is necessary for the formation of nanometric products with subsequent reaction.[1] Our present investigation confirms this, as will be discussed in more detail below.

Reactant powders which were milled separately (both milled at R = 250 rpm and CR = 21 but with t = 12 h for Si and t = 8 h for Mo) were reacted in the SPS with a power setting of 17% P_{max}. Figures 10(a)–10(c) show the corresponding results. Although preceded by a gradual change, an abrupt displacement occurred at 132 s and the maximum temperature recorded by the pyrometer is about 920 °C. The XRD pattern of the final product is shown in Fig. 10(c) which also includes the pattern corresponding to the starting mixture. It is evident that the reactants have completely transformed to α–MoSi$_2$ only (with minor amounts of Mo$_5$Si$_3$). The initially broad diffraction peaks of the elemental reactants are contrasted with the narrow peaks of the product, the latter suggesting a significant increase in crystallite size during synthesis. It should be emphasized that although the separately milled powders were milled at much stronger milling conditions (CR = 21 and t = 8–12 h) relative to the comilled case (3 h and CR = 14), they required a considerably longer time in the SPS to react. The comilled powders reacted within 2 s while the separately milled powders requires 132 s. This demonstrates the importance of interface formation during milling relative to crystallite size reduction.

Reactant samples containing small amounts of the product were investigated next. These powders correspond to milling conditions of R = 250 rpm, t = 7 h, and CR = 14. The XRD results of the product of SPS are shown in Fig. 11 for a condition of 17% P_{max}. The starting powder here contained some molybdenum disilicide, both in the α and β modifications. A sudden but smaller sample displacement (about 2 mm) occurred after only 1–2 s of the application of the electric power. The power was left on for a total time of 2 min during which no other changes were detected. The product contained mainly the tetragonal α–MoSi$_2$, but the presence of small
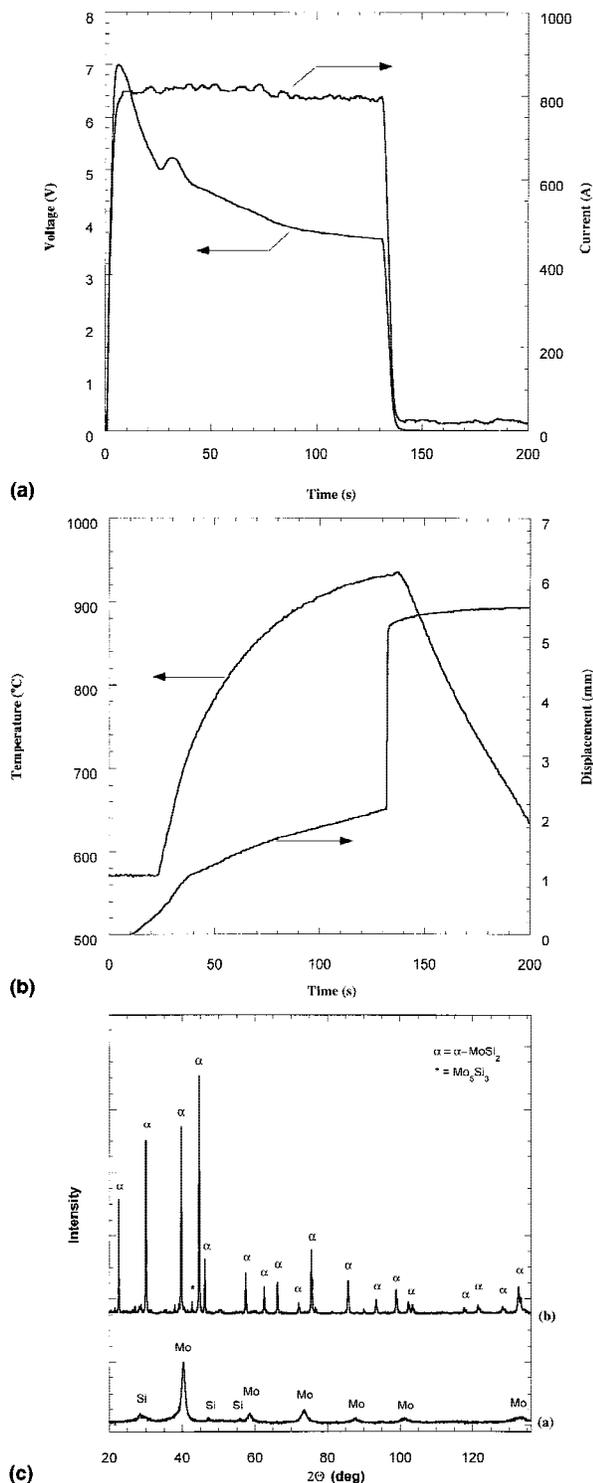
(a)

(b)

(c)

FIG. 10. (a) Voltage and current changes during SPS experiments ($P = 17\% \, P_{max}$) for Mo ($R = 250$ rpm; $t = 8$ h; CR = 21) + 2 Si ($R = 250$ rpm; $t = 12$ h; CR = 21) powders milled separately. (b) Temperature and sample displacement changes during SPS experiments ($P = 17\% \, P_{max}$) for Mo ($R = 250$ rpm; $t = 8$ h; CR = 21) + 2 Si ($R = 250$ rpm; $t = 12$ h; CR = 21) powders milled separately. (c) XRD patterns of the starting mixture (a) and of the SPS ($P = 17\% \, P_{max}$) final product (b) for Mo + 2 Si powders milled separately under the stated conditions in (a) and (b).

amounts of the hexagonal β–MoSi₂, Mo₅Si₃, and Mo was also detected. In this case, the product is in the nanometric range with the crystalline size of α–MoSi₂ evaluated to be about 140 nm. The relative density of the product is 94.8%.

The formation of the β modification of MoSi₂ during milling in our experiments is in agreement with previously reported studies.[6,7,9,11,12] In all of these reports, it was indicated that the formation of the β (high-temperature) phase follows the formation of the α (low-temperature) phase. Furthermore, an increase in milling time is reported to cause an increase in the β phase formation,[6,12] as was also observed in this work. Ma *et al.*[6] reported a transformation of α → β with increased milling as induced by the stored cold-work energy from milling. In the work of Bokhonov *et al.* the β phase was the main product after a 40-min milling.

The effect of an increase in the amount of the product in the reactant powders on the synthesis process was also evaluated. For this, powders which were milled for 2 h longer than in the previous case (i.e., $t = 9$ h) were used. The XRD results are shown in Fig. 12. The reaction took place after about 3–4 s with a sample displacement of about 0.5 mm, a much smaller value than in the previous cases (with $t = 7$ h). As in the previous case, however, the final product is a mixture of α–MoSi₂, β-MoSi₂, and unreacted Mo. However, the amount of the untreated Mo is significantly larger than in the case when the powders were milled for a shorter time. The amount of product in the reactants increases with milling time, as can be seen by comparing the lower scans of Figs. 11 and 12. The
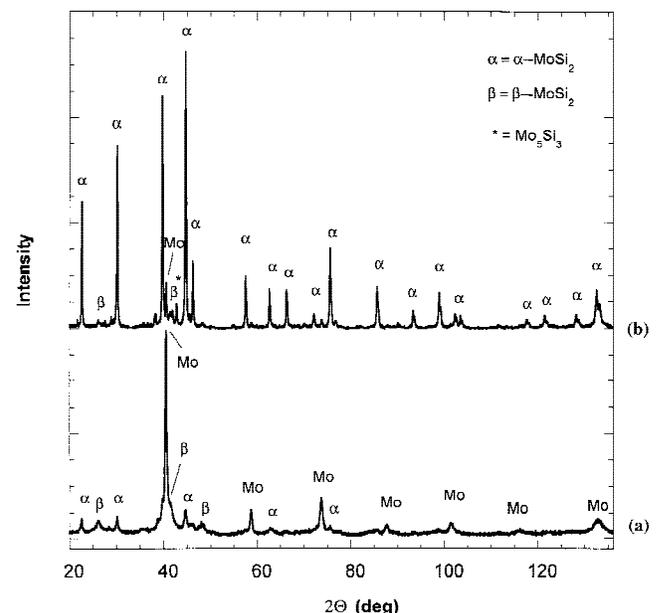

FIG. 11. XRD patterns of the starting mixture (a) and of the SPS final product (b) for Mo + 2 Si powders comilled under the conditions of $R = 250$ rpm, $t = 7$ h, CR = 14, and $P = 17\% \, P_{max}$.

formation of more product during milling decreases the driving force during synthesis and this explains the lower conversion of the sample that was milled longer. The combustion reaction seems to produce α–MoSi$_2$ while the β–MoSi$_2$ present in the reactant does not undergo a
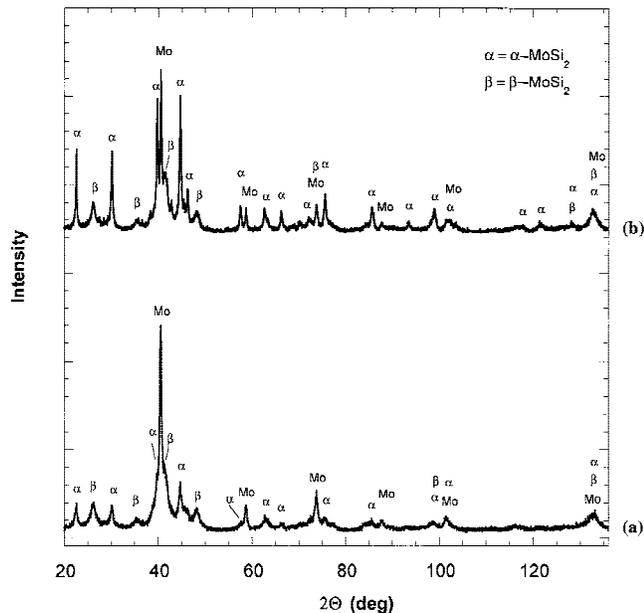

FIG. 12. XRD patterns of the starting mixture (a) and of the SPS ($P = 17\%\ P_{max}$) final product (b) for Mo + 2 Si powders comilled under the conditions of $R = 250$ rpm, $t = 9$ h, CR = 14, and $P = 17\%\ P_{max}$.
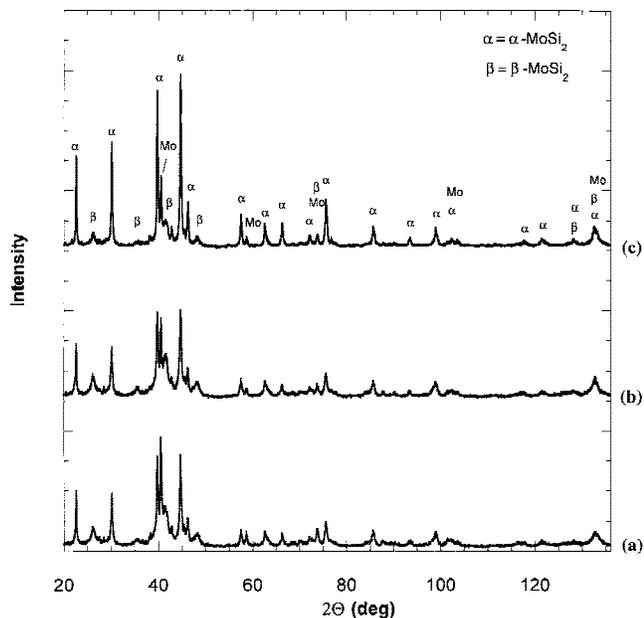

FIG. 13. XRD patterns of the SPS final product showing the effect of the powder (%) during synthesis: (a) 17, (b) 20, and (c) 25 for Mo + 2 Si powders comilled under the conditions $R = 250$ rpm, $t = 9$ h, and CR = 14.

transformation to the α form during the synthesis process. Yen reported that when milled reactant powders containing both α- and β–MoSi$_2$ were annealed at 750 °C, the product was mainly α–MoSi$_2$ but the β phase was still present.[9] But when annealing was done at 850 °C, the β phase transformed to the α phase. These observations are in contrast to those of Lee *et al.*[11] They reported that the β phase forms during annealing at 650 °C of milled powders which did not contain this phase prior to annealing. These results show that phase formation during milling and the effect of subsequent annealing on phase transformation are complex phenomena which required further investigations. Our observations show little effect of the SPS treatment on the β phase present in the milled powders. This would imply that the temperature is lower than 850 °C, on the basis of Yen's observations or that the time required for this phase transformation is much longer than the residence time in the SPS experiments.

The effect of the level of power on the conversion of the same sample ($R = 250$ rpm, $t = 9$ h, and CR = 14) was also investigated. Figure 13 shows the XRD of samples reacted at power levels of 17, 20, and 25% P_{max}. As the power increased, the amount of the unreacted Mo decreased while the amount of α–MoSi$_2$ increased.

IV. SUMMARY AND CONCLUSIONS

The one-step synthesis and consolidation of molybdenum silicide was investigated through mechanical and electric field activation. The effect of the parameters of mechanical activation (ball-milling) and field activation (SPS conditions) on the synthesis reaction and product cyrstallite size was studied. Molybdenum and silicon were milled separately or together (comilled) in a 1:2 atomic ratio. The effect of charge ratio (ball to powder mass ratio), milling time, and rotational speed on crystallite size was investigated for both cases. In addition the formation of new phases was monitored in the case of comilled powders.

Crystallite size decreased with an increase in all of the above-mentioned parameters, but in the ranges of the variables (milling time = 0–12 h, CR = 7–21, R = 250–300 rpm), the charge ratio had the most significant impact. When milled separately, the minimum molybdenum crystal size obtained in the range investigated is about 20 nm. On the other hand, the milling of silicon resulted in XRD peaks indicative of amorphous phase formation. For the case of comilling, the milling parameters under which product phase formation occurs were identified. Both the low-temperature, tetragonal phase α–MoSi$_2$ and the high-temperature, hexagonal phase β–MoSi$_2$ formed during milling. The minimum crystallite size for Mo before products formation during milling is about 125 nm and was obtained under the

conditions of $R = 250$ rpm, $t = 3$ h, and CR $= 14$. Si XRD peaks almost disappeared before product formation during the milling of the powders.

Mechanical activation played a major role in the subsequent synthesis by electric field activation. Milled powders showed a much higher reactivity. The formation of a product phase during milling was found to have a marked effect on the reaction and on the crystallite size of the product. Powders which were comilled, such that a product was formed, reacted to produce nanocrystalline MoSi$_2$. The results show that both α- and β-MoSi$_2$ form during milling but that only the α modification forms during the SPS reaction.

ACKNOWLEDGMENTS

REFERENCES

1. C. Gras, F. Charlot, E. Gaffet, F. Bernard, J.C. Neipce, Acta Mater. **47,** 2113 (1999).
2. H. Hahn and K.A. Padmanabhan, Philos. Mag. B **76,** 559 (1997).
3. Z.A. Munir, F. Charlot, F. Bernard, and E. Gaffet, U.S. Patent No. 6 200 515 (13 March 2001).
4. F. Charlot, F. Bernard, E. Gaffet, and Z.A. Munir, J. Am. Ceram. Soc. (in press, 2001).
5. J.W. Lee, Z.A. Munir, M. Shibuya, and M. Ohyanagi, J. Am. Ceram. Soc. (in press, 2001).
6. R.B. Schwarz, S.R. Srinivasan, J.J. Petrovic, and C.J. Maggiore, Mater. Sci. Eng., A **155,** 75 (1992).
7. E. Ma, J. Pagan, G. Cranford, and M. Atzmon, J. Mater. Res. **8,** 1836 (1993).
8. S.N. Patankar, S.Q. Xiao, J.J. Lewandowski, and A.H. Heuer, J. Mater. Res. **8,** 1311 (1993).
9. B.K. Yen, J. Appl. Phys. **81,** 7061 (1997).
10. G.T. Fei, L. Liu, X.Z. Ding, L.D. Zhang, and Q.Q. Zheng, J. Alloys Compd. **229,** 280 (1995).
11. P.Y. Lee, T.R. Chen, J.L. Yang, and T.S. Chin, Mater. Sci. Eng. A, **192/193,** 556 (1995).
12. B.B. Bokhonov, I.G. Kostanchuk, and V.V. Boldyrev, J. Alloys Compd. **218,** 190 (1995).
13. P. Sajgalik, M. Hnatko, F. Lofaj, P. Hvizdos, J. Dusza, P. Warbichler, F. Hofer, R. Riedel, E. Lecomte, and M.J. Hoffmann, J. Eur. Ceram. Soc. **20,** 453 (2000).
14. C.E. Borsa, H.S. Ferreira, and R.H. Kiminami, J. Eur. Ceram. Soc. **19,** 615 (1999).
15. D.S. Cheong, K.T. Hwang, and C.S. Kim, Composites, Part A **30,** 425 (1999).
16. J.M. Wu and Z.Z. Li, J. Alloy Compd. **299,** 9 (2000).
17. L. Gao, H.Z. Wang, J.S. Hong, H. Miyamoto, K. Miyamoto, Y. Nishikawa, and S.D. Torre, J. Eur. Ceram. Soc. **19,** 609 (1999).
18. L. Gao, H.Z. Wang, J.S. Hong, H. Miyamoto, K. Miyamoto, Y. Nishikawa, and S.D. Torre, Nanostruct. Mater. **11,** 43 (1999).
19. Z.A. Munir, I.J. Shon, and K. Yamazaki, US Patent No. 5 794 113 (11 August 1998).
20. I.J. Shon, Z.A. Munir, K. Yamazaki, and K. Shoda, J. Am. Ceram. Soc. **79,** 1875 (1996).
21. G.K. Williamson and W.H. Hall, Acta Metall. **1,** 22 (1953).
22. J.I. Langford, in *Accuracy in Powder Diffraction II,* edited by E. Prince and J.K. Stalick (NIST Publ. **846,** Gaithersburg, MD, 1992), pp. 110–126.
23. M. Tokita, in *Proceedings of NEDO International Symposium on Functionally Graded Materials,* Tokyo, Japan, October 21–22 (1999), pp. 23–33.
24. H.B. Huntington, in *Diffusion in Solids,* edited by A.S. Nowick and J.J. Burton (Academic Press, New York, 1975), pp. 303–352.
25. R. Orrù, J. Garay, G. Cao, and Z.A. Munir (unpublished).